

## COMMUNICATIONS

# Application of Interlaced Fourier Transform to Echo-Planar Spectroscopic Imaging\*

GREGORY METZGER AND XIAOPING HU

*Center for Magnetic Resonance Research and Department of Radiology, Medical School, University of Minnesota, Minneapolis, Minnesota 55455*

Received November 25, 1996

To reduce the time needed for spatial encoding in magnetic resonance spectroscopic imaging, echo-planar-based high-speed techniques were introduced (1–3) and implemented (4, 5). In echo-planar spectroscopic imaging (EPSI), the temporal sampling interval, determined by the period of the readout–gradient alternation, limits the achievable spectral bandwidth. This limitation is exacerbated by the current implementation of EPSI, which separates the odd and the even echoes in the reconstruction. In this Communication, a new method of reconstruction based on the interlaced Fourier transform is described and experimentally demonstrated. By utilizing both the odd and even echoes, the method is able to double the spectral bandwidth achievable with existing reconstruction approaches.

Since it was first introduced in 1982 (6), magnetic resonance spectroscopic imaging has been developed into a widely used method for localized NMR spectroscopy. However, a major limitation of MRSI is the long acquisition time imposed by the need of phase encoding for all spatial dimensions and the limited signal-to-noise ratio (SNR) of the metabolite peaks. To reduce the acquisition time, echo-planar spectroscopic imaging methods that utilize an alternating gradient along one of the spatial dimensions were introduced (1–3). By reducing the phase-encoding dimension by one, EPSI can be used for fast two-dimensional spectroscopic imaging when the SNR is not a limiting factor and for practical three-dimensional spectroscopic imaging. Recent implementation of EPSI (4, 5) has demonstrated its utility for *in vivo* studies, particularly for spectroscopic imaging in three spatial dimensions (4).

As illustrated in a schematic diagram of a two-dimensional EPSI sequence (Fig. 1a), an alternating gradient is applied along one of the spatial dimensions (the readout direction), generating a series of gradient echoes that are sampled. The spatial encoding along the readout direction is achieved with the alternating gradient while phase encoding is used along

the other spatial dimension. In the rest of the paper, with no loss of generality, only the readout direction is considered for simplicity. The data-acquisition process covers a portion of the  $k$ - $t$  space, consisting of the spatial frequency along the readout direction and time, in the manner shown in Fig. 1b. It is evident from Fig. 1b that the sampling interval in time is determined by the alternation period of the readout gradient, the limits of which are dictated by the gradient hardware. Therefore, the spectral bandwidth in EPSI can be hardware limited. This problem is particularly severe for many existing scanners without high-performance gradients and for nuclei having a large chemical-shift range (e.g., C-13). To alleviate this problem, an approach using multiple acquisitions with a slight shift in echo time (3) was described; this approach, however, increased the acquisition time by a factor proportional to the number of acquisitions. More recently, a selective-excitation approach was introduced to reduce this problem by restricting the bandwidth of the excited signal (7); this approach is cumbersome to use and may not be feasible when the repetition time is not long enough to accommodate more than one data-acquisition window or when multiple slices are desired.

As is evident in Figs. 1b and 1c, the sampling in time is not uniform for most of the  $k$ -space points. This sampling nonuniformity could lead to spectral aliasing. To avoid this problem, a recent implementation of EPSI separates the odd echoes and the even echoes in the reconstruction and combines the reconstructed spectra later (4, 5). Such a reconstruction approach reduces the theoretically available spectral bandwidth permitted by the gradient hardware by a factor of 2. Figure 1b also indicates that the temporal locations of the samples are  $k$ -space dependent; this difference can result in chemical-shift artifacts. In this Communication, we describe a technique that allows the incorporation of both odd and even echoes in the reconstruction and removes temporal inconsistency between  $k$ -space points. Consequently, the present technique permits the realization of the theoretical spectral bandwidth, effectively doubling the spectral band-

\* Work supported by the National Institutes of Health (Grant RR08079).

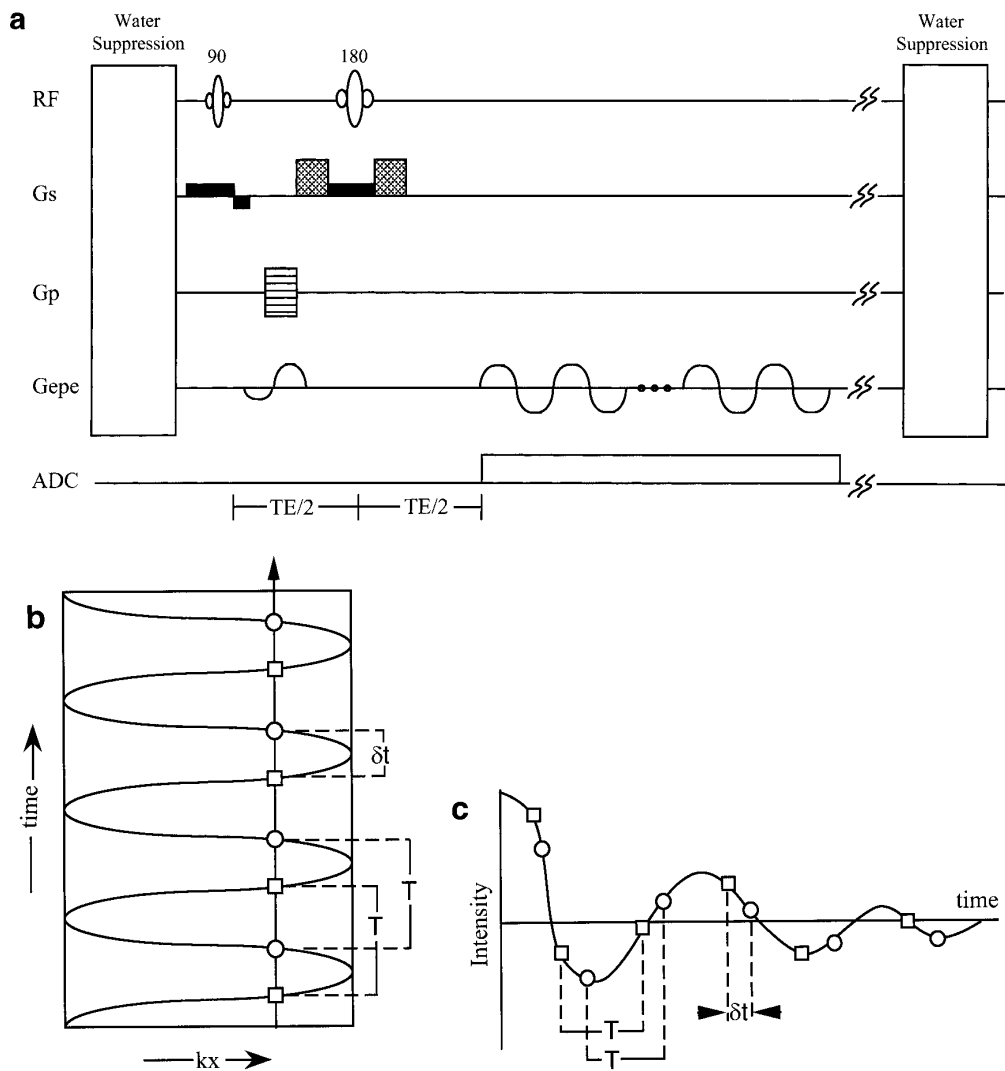


**FIG. 1.** (a) The diagram of a typical two-dimensional EPSI sequence. In this sequence, the acquired signal is phase-encoded in Gp direction and echo-planar-encoded in the Gepe direction. (b) A representation of the traversal of the  $k$ - $t$  space achieved during the data acquisition in an EPSI sequence. (c) A schematic representation of the measured signal along the time axis in the  $k$ - $t$  space as shown in (b). Note that the timing parameters  $T$  and  $\delta t$  are indicated in both (b) and (c).

width available with the current implementation, and eliminates chemical-shift artifacts. This is achieved by using the interlaced Fourier transform along the time domain and by appropriate phase shifting in the spectral domain. In the actual implementation, the  $k$ -space trajectory is experimentally determined to provide data-acquisition timing needed by the interlaced Fourier transform.

We now examine the temporal coverage of a single  $k$ -space point as shown in Figs. 1b and 1c. In general, the time interval between the odd and even data points ( $\delta t$ ) is not equal to the interval between the even and the odd points ( $T - \delta t$ ) and is dependent on  $k$ ; however, the time between odd (or even) points,  $T$ , is constant and independent of the  $k$ -space location. Data sampled in this manner call for the use of the interlaced Fourier transform and provide an effective

bandwidth determined with a sampling interval of  $T/2$ . Specifically, the discrete Fourier transform of the odd points,  $o(\omega, k)$  and that of the even points,  $e(\omega, k)$ , are first calculated separately and combined according to

$$g(\omega, k) = \frac{-e^{i\alpha 2\pi\delta t/t}}{1 - e^{i\alpha 2\pi\delta t/t}} o(\omega, k) + \frac{e^{-i\omega\delta t}}{1 - e^{i\alpha 2\pi\delta t/t}} e(\omega, k)$$

$$h(\omega, k) = \frac{1}{1 - e^{i\alpha 2\pi\delta t/t}} o(\omega, k) - \frac{e^{-i\omega\delta t}}{1 - e^{i\alpha 2\pi\delta t/t}} e(\omega, k), \quad [1]$$

where  $\alpha = -1$  for  $\omega \geq 0$ ,  $\alpha = 1$  for  $\omega < 0$ , to give rise to  $h(\omega, k)$  and  $g(\omega, k)$ , which are subsequently concatenated to form an extended spectrum,  $\tilde{F}(\omega, k)$ , using

$$\left. \begin{aligned} \tilde{F}(\omega, k) &= h\left(\omega + \frac{\Omega}{2}, k\right) & -\frac{\Omega}{2} \leq \omega < -\frac{\Omega}{4} \\ \tilde{F}(\omega, k) &= g(\omega, k) & -\frac{\Omega}{4} \leq \omega < \frac{\Omega}{4} \\ \tilde{F}(\omega, k) &= h\left(\omega - \frac{\Omega}{2}, k\right) & \frac{\Omega}{4} \leq \omega < \frac{\Omega}{2} \end{aligned} \right\} \text{where } \Omega = \frac{2}{T}. \quad [2]$$

Since the sampling for each  $k$ -space location starts at a slightly different time, the spectra reconstructed based on Eq. [2] are inconsistent and cannot be used for the subsequent analysis along the  $k$  direction. To remove this inconsistency, a phase modulation, linear along the chemical-shift direction and proportional to the time shift,  $\varepsilon = (T - \delta t)/2$ , is applied to  $\tilde{F}(\omega, k)$ :

$$F(\omega, k) = \tilde{F}(\omega, k)e^{-i2\pi\varepsilon\omega}. \quad [3]$$

The  $F(\omega, k)$  in Eq. [3], spanning a  $k$ - $\omega$  space, can be analyzed for each fixed  $\omega$ . The processing along  $k$  space consists of regridding of nonuniformly sampled data (8), time reversal of the even echoes, and spatial Fourier transformation.

To demonstrate this approach, an EPSI sequence was implemented on a Siemens Vision scanner (Siemens Medical Systems, Iselin, New Jersey) whose gradient system is capable of a maximum gradient of 25 mT/m with a sinusoidal ramping time of 300  $\mu$ s. In this sequence, a spin-echo excitation (with both the 90° and 180° pulses slice selective) is preceded by chemically selective water-suppression pulses (9), and the second half of the echo is spatially encoded with echo-planar encoding in one spatial dimension and phase encoding in the other (Fig. 1a). For the echo-planar encoding, the readout gradient consisted of 512 pairs of alternating gradient lobes, each having a 300  $\mu$ s quarter-sine wave rampup, a 650  $\mu$ s flat portion, and a 300  $\mu$ s quarter-sine wave rampdown. The 512 pairs correspond to 1024 time points at each  $k$ -space location, with an effective sampling interval of 1.25 ms (or spectral bandwidth 800 Hz when both the odd and even echoes are used as described in this Communication). The total sampling time was 1.28 s. Within each gradient lobe, 200 complex data points were sampled and interpolated to a matrix size of 128  $k$ -space points.

Theoretically, the traversal of the  $k$ - $t$  space can be derived according to the sequence design, providing the timing information needed for the interlaced Fourier transformation and the  $k$ -space coverage for regridding. In practice, imperfections in gradient hardware and system timing make the theoretical determination of the  $k$ - $t$  trajectory inaccurate. To avoid this problem, the trajectory in the  $k$ - $t$  space is experi-

mentally determined using a preencoding scheme that was previously described (10). The  $k$ - $t$  trajectory derived from this measurement is shown in Fig. 2. The  $k$ - $t$  trajectory is used first to determine the relative shift between the onset of the echo-planar gradient and the start of data acquisition, which is used to preshift the EPSI data in time before further processing. More importantly, the  $k$ - $t$  trajectory is used to match the odd echoes and even echoes as follows. Gradient hardware and timing imperfections result in discrepancies in the  $k$ -space locations between the odd-echo data and the even-echo data. To avoid this problem, the data points of the even echoes are interpolated using a spline routine so that the even-echo data are adjusted to fall on the  $k$ -space locations of the odd-echo data, and the sampling time of the interpolated data is determined by linear interpolation of original  $k$ -space sampling times. The  $\delta t$  values are calculated based on the original sampling times of the odd-echo data and the calculated sampling times of the interpolated even-echo data. In the reconstruction along the  $k$ -space direction, the  $k$ - $t$  trajectory for the odd echo is used in regridding the data.

Experimental data were obtained on a phantom consisting of two cylinders placed concentrically. The inner cylinder contained a solution of lactate and acetate while the outer

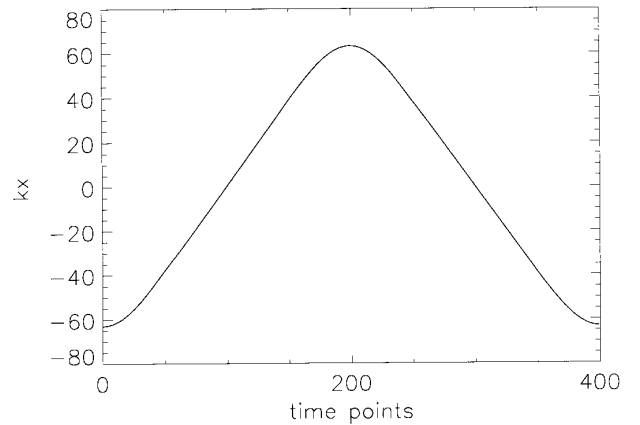
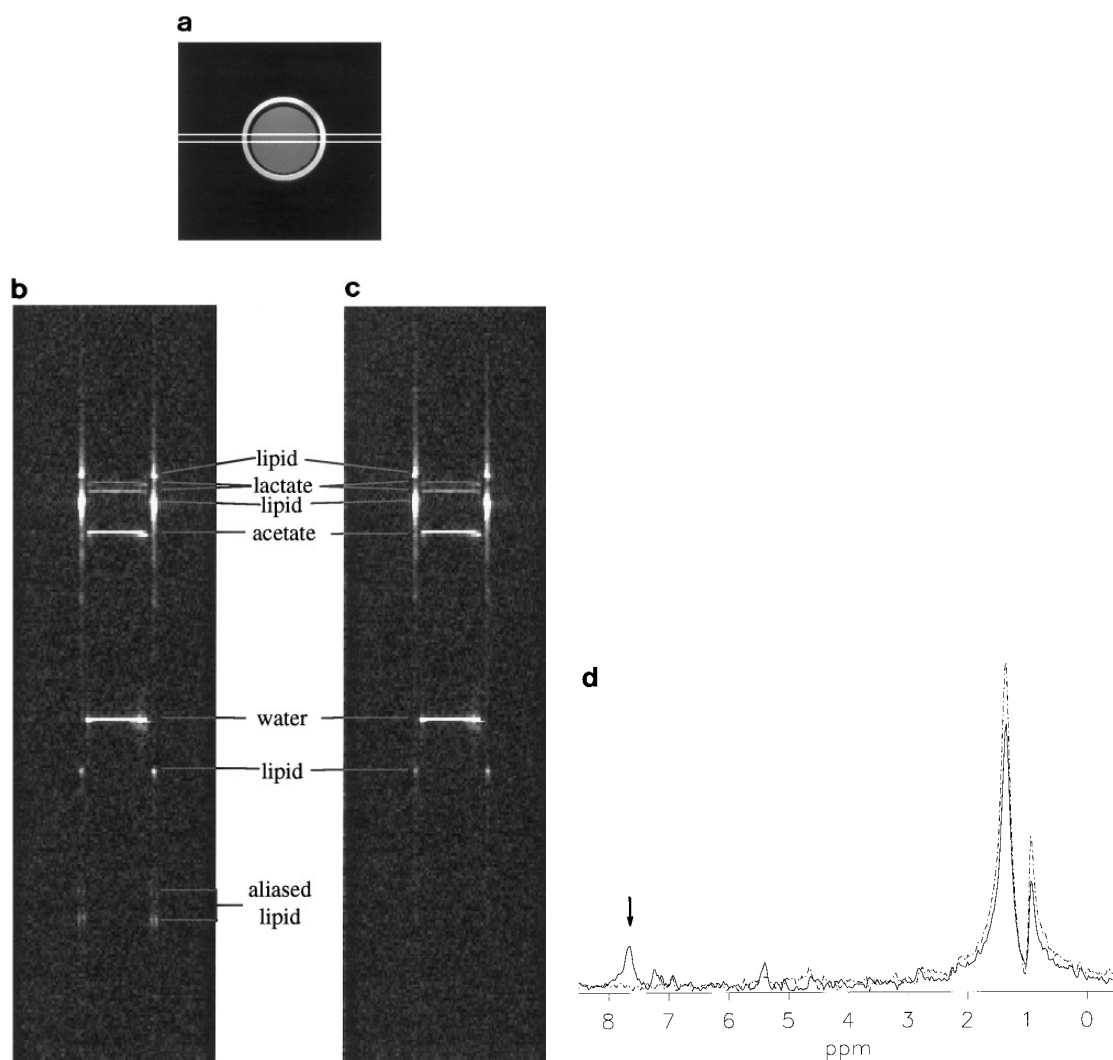


FIG. 2. The experimentally determined  $k$ - $t$  space trajectory. The upward half corresponds to the odd echoes (the positive gradient lobe) and the downward half corresponds to the even echo (the negative gradient lobe).



**FIG. 3.** (a) The anatomic image of the two-dimensional slice studied by the EPSI experiment. A one-dimensional column for the data presented in (b) and (c) is marked. (b) A slice of EPSI data reconstructed without using the interlaced FT method. (c) The slice of EPSI data reconstructed with the interlaced FT method. In both (b) and (c), the slice was taken along the echo-planar encoding direction and the spectral direction. The spectral dimension is vertical and the spatial axis is horizontal. (d) Spectra from a pixel in the outer cylinder obtained with interlaced FT (dashed) and without the interlaced FT (solid). The aliasing in the spectra obtained without the interlaced FT is indicated by the arrow. These spectra were processed with a 5 Hz line broadening.

cylinder contained cooking oil. The experiments were conducted with a TR/TE of 1500/165 ms. A field of view of  $24 \times 24$  cm was used with a slice thickness of 10 mm.

The result of the experimental study is presented in Fig. 3. Panel (a) shows the anatomic image of the phantom and a horizontal column indicating the location of the data shown in panels (b) and (c). A slice along the echo-planar encoding direction (horizontal) and the spectral direction (vertical) of the reconstructed EPSI data using the interlaced method is illustrated in panel (c), while the result of processing without the interlaced FT is shown in panel (b). The slice from the interlaced reconstruction clearly depicts the spatial and spectral content consistent with the materials in the

phantom and is free of artifacts in both the spatial and spectral directions. In contrast, the result reconstructed without the interlaced FT exhibits aliasing of the lipid and lactate resonances to  $\sim 7.7$  ppm. Figure 3d illustrates spectra in the outer cylinder from the data presented in Figs. 3b and 3c. The spectrum from the interlaced reconstruction (dashed) captures the full bandwidth theoretically achievable. In fact, the absence of the aliased version of the lipid signal clearly demonstrates the performance of the interlaced approach. In the spectrum obtained without using the interlaced FT and the related data interpolation based on the  $k-t$  measurement (solid), the aliasing of the resonance peaks of the lipid is apparent.

The interlaced Fourier transform has previously been used for the reconstruction of echo-planar images (11). The work presented in this paper represents the first successful demonstration of its use for echo-planar spectroscopic imaging. It should be noted that the interlaced approach could be more sensitive to noise in the measured data when  $\delta t$  becomes small. This is the case for  $k$ -space locations away from the origin. However, since these points usually correspond to regions with a high degree of oversampling in the  $k$  space, the noise sensitivity of the interlaced FT is offset by data averaging and usually does not lead to a significant problem.

The  $k-t$  measurement employed in this study was important for the accurate implementation of the interlaced Fourier transform. On our system, the  $k$ -space trajectory was not significantly distorted since eddy-current effects were negligible. Nevertheless, this measurement was found to be necessary. On systems where the eddy-current effect is severe, the  $k$ -space trajectory measurement will be more beneficial.

The linear phase correction in the frequency domain as used here can also facilitate the averaging of separate reconstructions of the odd and even echoes because it can effectively shift the odd- and even-echo points to identical temporal locations. Such an approach makes the averaging of absorption spectra straightforward and provides the optimal SNR.

In conclusion, a new reconstruction method for EPSI is described and demonstrated. This method allows the use of the odd and even echoes in the spectral reconstruction so that the spectral bandwidth is not sacrificed due to the separation of the echoes. Experimental results show that the method, when combined with  $k$ -space trajectory calibration, is robust. With the expanded bandwidth, this method will make EPSI applicable to systems without high-performance gradients and to nuclei with a broader chemical-shift range.

## REFERENCES

1. P. Mansfield, *Magn. Reson. Med.* **1**, 370 (1984).
2. S. Matsui, K. Sekihara, and H. Kohno, *J. Am. Chem. Soc.* **107**, 2817 (1985).
3. S. Matsui, K. Sekihara, and H. Kohno, *J. Magn. Reson.* **67**, 476 (1986).
4. S. Posse, C. DeCarli, and D. Le Bihan, *Radiology* **192**, 733 (1994).
5. S. Posse, G. Tedeschi, R. Risinger, R. Ogg, and D. Le Bihan, *Magn. Reson. Med.* **33**, 34 (1995).
6. T. R. Brown, B. M. Kincaid, and K. Ugurbil, *Proc. Natl. Acad. Sci. U.S.A.* **79**, 3523 (1982).
7. S. Hirata, Y. Bito, and E. Yamamoto, *Magn. Reson. Med.* **35**, 611 (1996).
8. H. Bruder, H. Fischer, H. E. Reinfelder, and F. Schmitt, *Magn. Reson. Med.* **23**, 311 (1992).
9. R. J. Ogg, P. Kingsley, and J. Taylor, *J. Magn. Reson. B* **104**, 1 (1994).
10. A. Takahashi and T. Peters, *Magn. Reson. Med.* **34**, 446 (1995).
11. K. K. H. Sekihara, *Magn. Reson. Med.* **5**, 485 (1987).